A Multitime Circuit Formulation for Closely Spaced Frequencies

Jaijeet Roychowdhury

University of Minnesota, Minneapolis, MN

Received 17 October 2004; accepted 23 December 2004

ABSTRACT: Verifying circuits with two or more closely-spaced driving frequencies is important in RF and wireless communications, for example, in the design of down-conversion mixers. Existing steady-state calculation methods, like harmonic balance, rely on Fourier series expansions to find the difference-frequency components typically of interest. Time-domain methods are, however, better suited for circuits with strong nonlinearities such as switching. Towards this end, we present a purely time-domain method for direct computation of difference tones in closely-spaced multitone problems. Our approach is based on multiple artificial time scales for decoupling the tones driving the circuit. Our method relies on a novel multitime reformulation that expresses circuit equations directly in terms of time-scales corresponding to difference tones. We apply the new technique to an RF-CMOS mixer to predict baseband bit-streams and down-conversion gain and distortion, in two orders of magnitude less CPU time than traditional time-stepping simulation. © 2005 Wiley Periodicals, Inc. Int J RF and Microwave CAE 15: 382–393, 2005.

Keywords: simulation; RF; multitone; multitime methods

I. INTRODUCTION

RF sections of wireless-communication systems typically involve one or more stages of frequency conversion, with frequency tones that are either widely separated, or very closely spaced. While frequency up-conversion in transmitters involves widely separated frequencies, down-conversion circuits in receivers are typically driven by two or more very closely spaced frequencies. For example, a direct-conversion cellphone could feature tones at 1.8 GHz, spaced only a few Mhz or 100s of kHz apart. The difference frequencies are of primary interest in receiver design and verification, since they carry the information being received; hence, design and verification tools must necessarily deal with the small frequencies together with the large ones.

As is well known, simulating circuits with disparate frequencies using time-stepping methods, such as those used for transient simulation in SPICE [8, 12] and similar tools, can be very inefficient, particularly when the time-varying steady-state solution is desired. Better methods exist for both widely-separated and closely-spaced driving tones. An important technique that is useful for both situations is harmonic balance (HB) (see, for example, [3, 5, 7]). HB expands all time-varying waveforms in the circuit in Fourier series components featuring the driving tones, their harmonics, and intermodulation products (that is, mixing terms or "mix components"). Since sum and difference frequencies appear explicitly in the mix components, HB is able to accommodate both widely-separated and closely-spaced driving tones naturally. Unfortunately, Fourier series expansions are also the Achilles' heel of HB, for they are ill-suited to wave-

Correspondence to: J. Roychowdhury; e-mail: jr@ece.umn.edu.
DOI 10.1002/mmce.20094
Published online 9 May 2005 in Wiley InterScience (www.interscience.wiley.com).

forms with sharp corners or peaks. Such waveforms arise in modern integrated-RF designs, such as switching RF circuits, desirable for their low power and noise characteristics. In these situations, that is, when strong nonlinearities are encountered, time-domain methods are usually preferred over frequency-domain ones like HB.

Purely time-domain methods for steady-state and RF calculations have, until recently, been limited to single-tone problems, with shooting and its variants commonly used (for example, [2, 9, 15]). Recently, artificial time scale approaches [3, 13] have addressed the multitone case, resulting in purely time-domain methods for quasi-periodic steady state and envelope simulation. So far, however, these techniques have concentrated only on the case of widely-separated driving tones.

In this work, we extend multitime approaches to the case of closely-spaced driving tones. The key enabler towards this end is our ability to reformulate time-domain circuit equations driven by two or more closely spaced tones directly in terms of time scales corresponding to difference tones. As it involves shearing or rotation of the time scales corresponding to the closely-spaced driving tones, this reformulation procedure is quite generally applicable to any waveform shape at either the driving tones or the difference tones. Finding the solution at the difference-frequency time scales makes it possible to obtain, directly, the shape of baseband or down-converted information signals (such as bit streams) in the time domain.

The reformulated multitime equations are discretized along the artificial time dimensions to obtain a purely time-domain solution technique, similar to the MFDTD and TD-ENV methods in [13]. Quasi-periodic and envelope-type solutions can both be found. The reformulated equations also result in variants of mixed frequency-time (MFT) techniques reported in [6, 13].

We present applications of a new technique to balanced and unbalanced switching mixer circuits for direct-conversion receivers, similar to those reported recently in [10, 16]. We are able to obtain, directly, time-domain waveforms for sections of bit streams downconverted to baseband. Using pure-tone driving excitations, we are also able to obtain down-conversion gain and distortion figures. This new method is faster by about two orders of magnitude than periodic steady-state computation using single-time shooting.

Although this new technique is demonstrated on RF communication circuits in this article, the proposed method can be applied generally to other systems featuring closely spaced tones, such as power-conversion circuits and electro-optical communication systems.

In the remainder of this article, we first describe schemes for reformulating the circuit equations in terms of difference-frequency time scales in section II and then outline time-domain schemes for numerical solution in section III. In section IV, we describe the application of the new technique to the aforementioned circuits, and provide interpretations of the results obtained.

II. DIFFERENCE TIME-SCALE FORMULATION

A. Multitime Circuit Equations

We first recall the basic concepts of multitime circuit formulations, following the approach in [13]. The equations of the circuit are represented as

$$\dot{q}(x(t)) + f(x(t)) + b(t) = 0, \tag{1}$$

where $q(\cdot)$ represents the linear and nonlinear charge/flux terms, $f(\cdot)$ the conductive terms, $b(t)$ the excitation, and $x(t)$ the unknowns (voltages and currents) in the circuit. When the excitation is multitone (whether closely or widely spaced), $b(t)$ can be expressed in terms of multivariate functions involving several artificial time scales. For example, a two-tone signal may be expressed as

$$b(t) = \hat{b}(t, t), \tag{2}$$

where

$$\hat{b}(t_1, t_2) = \hat{b}(t_1 + T_1, t_2 + T_2) \tag{3}$$

is periodic in each of its two arguments, for some periods T_1 and T_2. The two tones of excitation are $f_1 = (1/T_1)$ and $f_2 = (1/T_2)$; they are widely separated if $f_1 \gg f_2$ (or vice-versa). If the tones are closely spaced, then typically, $f_1 \sim f_2 \gg |f_1 - f_2|$.

In [13], it has been shown that when the tones are widely separated, the multitime representation (3) can be represented far more compactly, in terms of numerical samples, than the normal single-time form (2). This fact is applied towards solving the circuit equations (1), by assuming that the circuit unknowns $x(t)$ can also be expressed in a numerically compact multitime form similar to (3). Finding this multitime solution directly involves solution of the following multitime partial differential equation (MPDE) corresponding to (1):

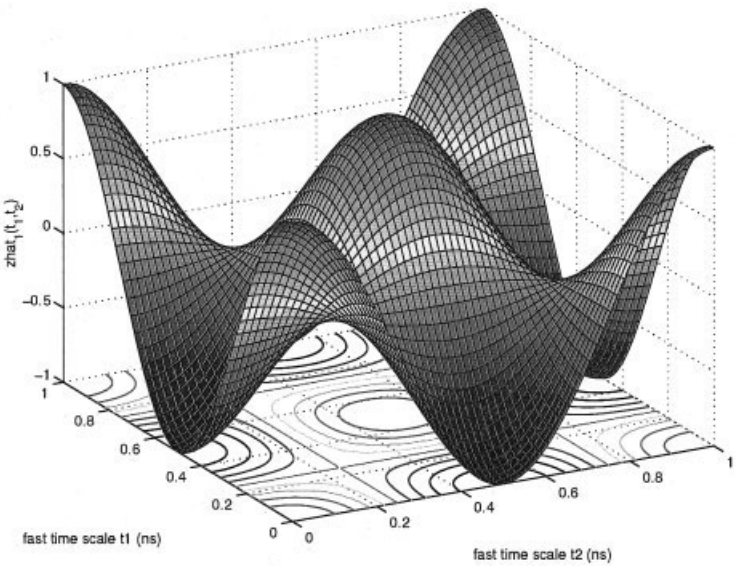

Figure 1. $\hat{z}_1(t_1, t_2)$.

$$\frac{\partial q(\hat{x}(t_1, t_2))}{\partial t_1} + \frac{\partial q(\hat{x}(t_1, t_2))}{\partial t_2} + f(\hat{x}(t_1, t_2)) + \hat{b}(t_1, t_2) = 0. \quad (4)$$

In eq. (4), $\hat{x}(t_1, t_2)$ is the multitime representation of $x(t)$ that is sought. It has been shown that if $\hat{x}(t_1, t_2)$ satisfies (4), then $x(t) = \hat{x}(t, t)$ solves the original circuit equations (1). Regardless of whether the tones in the circuit are separated or not, this basic fact always holds.

When the driving tones are in fact widely separated, for example, $T_1 \ll T_2$, solving the MPDE (4) is preferred over solving (1) for two reasons. First, $\hat{b}$ and $\hat{x}$ can be represented much more efficiently than their single-time counterparts; and second, the t_1 and t_2 variations of the solution $\hat{x}(t_1, t_2)$ directly provide information of interest, namely, the slowly-varying envelope and the detailed shape of the fast variations at any point under the envelope.

B. Closely Spaced Tones

When the tones are closely spaced, that is, $T_1 \sim T_2$, the MPDE (4) as it stands is still perfectly valid,

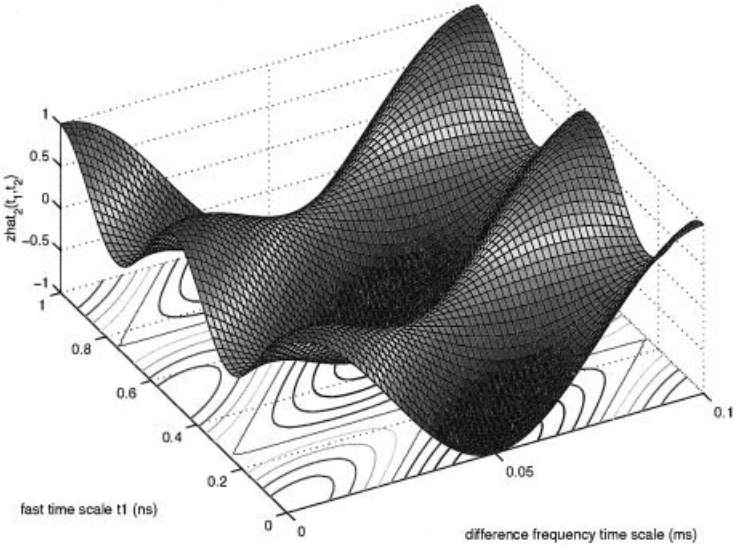

Figure 2. $\hat{z}_2(t_1, t_2)$.

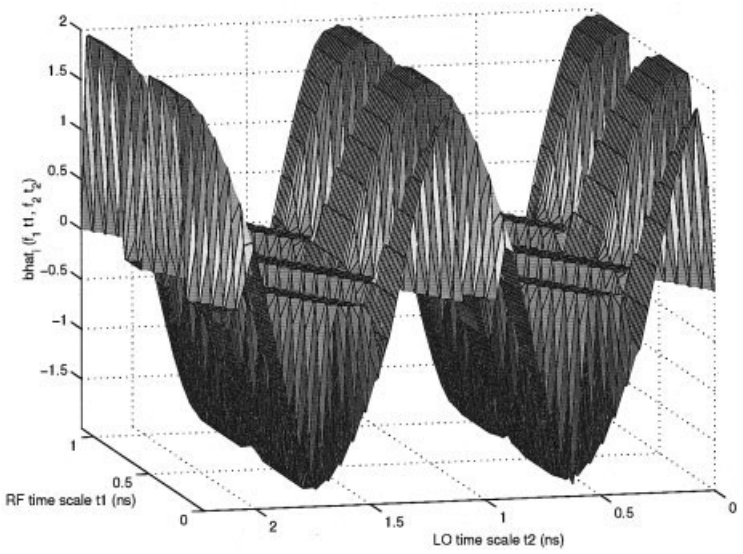

Figure 3. $\hat{b}_i(f_1 t_1, f_2 t_2)$.

however it is not immediately useful as in the widely separated case, even though $\hat{b}$ and $\hat{x}$ are still numerically far more compact than their single-time counterparts. The reason for this is that the frequencies of interest are typically difference frequencies, such as $f_1 - f_2$, $2f_1 - f_2$, and so on. The difference frequencies are much smaller than f_1 or f_2, and manifest themselves as baseband signals or as slow envelopes riding on much faster waveforms. The multitime solution $\hat{x}$ does not directly provide the slow waveforms at these frequencies. As a concrete example, consider the ideal mixing operation

$$z(t) = x(t)\,y(t), \tag{5}$$

where $x(t) = \cos(2\pi f_1 t)$ and $y(t) = \cos(2\pi f_2 t)$, with $f_1 = 1$ GHz and $f_2 = f_1 - 10$ kHz. In other words, the two tones f_1 and f_2 are very closely spaced, with the difference tone $f_1 - f_2 = 10$ kHz being much smaller. The mixing operation (5) generates this difference tone explicitly, since

$$z(t) = \tfrac{1}{2}\left[\cos(2\pi \times 10\,\text{kHz} \times t) + \cos(2\pi(f_1 + f_2)t)\right], \tag{6}$$

and the high frequency component at $f_1 + f_2$ is usually eliminated by separate filtering. The multitime representation of $z(t)$, given by

$$\hat{z}_1(t_1, t_2) = \cos(2\pi f_1 t_1)\cos(2\pi f_2 t_2), \tag{7}$$

does not directly provide this difference-frequency component.

For a multitime method to be practically useful in the case of closely-spaced driving tones, it must be capable of directly solving for these slow waveforms in the time domain. We now outline how this can be achieved. The key insight is to realize that a given $\hat{b}$ satisfying (2) is not unique, that is, there are many functions $\hat{b}$, with different T_1 and T_2 values in (3), providing the same $b(t)$ given by (2). We illustrate this with our ideal mixing example. For convenience, we first define

$$\hat{z}_s(t_{1s}, t_{2s}) = \cos(2\pi t_{1s})\cos(2\pi t_{2s}) \tag{8}$$

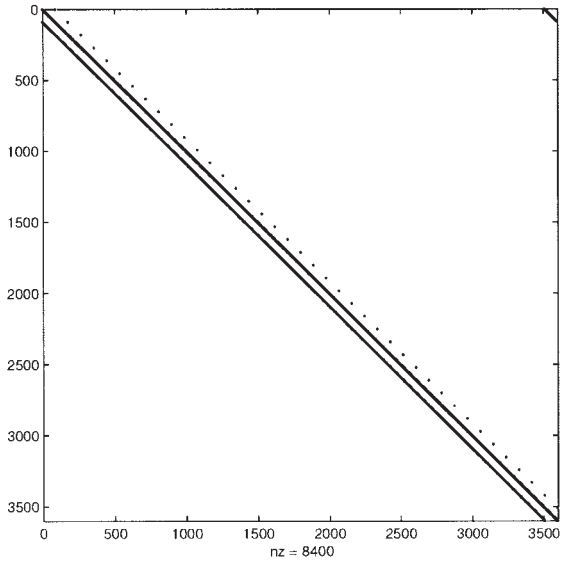

Figure 4. Jacobian matrix structure.

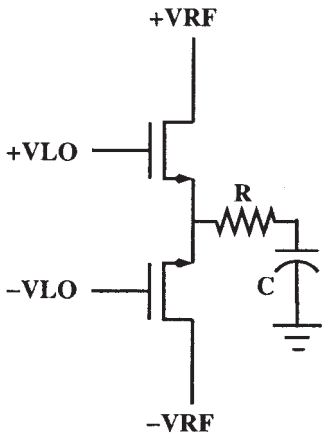

Figure 5. Unbalanced CMOS down-conversion mixer.

to be a scaled multitime representation of $z(t)$, periodic with period 1 in both its arguments. $\hat{z}_1$ in (7) can be expressed in terms of this as follows:

$$\hat{z}_1(t_1, t_2) = \hat{z}_s(f_1 t_1, f_2 t_2). \tag{9}$$

Note that $\hat{z}_1$ above, with periods $T_1 = (1/f_1)$ and $T_2 = (1/f_2)$ very similar to each other, does not provide difference-frequency information directly; but as always required, it satisfies $z(t) = \hat{z}(t, t)$.

If we now define a difference frequency of interest to be

$$f_d = f_1 - f_2 = 10 \text{ kHz}, \tag{10}$$

and the corresponding period $T_d = (1/f_d) = 0.1$ ms, we can devise a new multitime representation:

$$\hat{z}_2(t_1, t_2) = \hat{z}_s(f_1 t_1, f_1 t_1 - f_d t_2). \tag{11}$$

Note that $\hat{z}_2$ is periodic with respect to t_1 and t_2, with periods T_1 and T_d, respectively; hence, its changes along t_2 capture variations corresponding to difference-frequency time scales. Furthermore, it continues to satisfy the requirement $z(t) = \hat{z}_2(t, t)$; hence, is as relevant to the underlying one-time problem as $\hat{z}_1(t_1, t_2)$. $\hat{z}_1$ and $\hat{z}_2$ are plotted in Figures 1 and 2, respectively; note the explicit variation in the difference time scale (spanning 0.1 ms) in the latter.

Note that the arguments $(f_1 t_1, f_1 t_1 - f_d t_2)$ in (11) can be interpreted geometrically as scaling and shearing of the original time scales (t_{1s}, t_{2s}) in (8). Furthermore, numerical compactness of representation is not affected by the shearing, as can be seen in Figure 2. Hence, time-sheared multitime representations for $\hat{b}$ and $\hat{x}$ can be applied to the MPDE (4), and a solution obtained directly in terms of the slow difference-frequency time scale of interest.

We also note that eq. (10) is only one way of defining a difference-frequency time scale; depending on the application, other difference frequencies should be used. For example, in the balanced mixer circuit in section IV, the local oscillator frequency $f_1 = 450$ MHz is doubled internally within the circuit and then mixed with the information-carrying tone close to 900 MHz. Hence, the difference frequency of interest (at baseband) is given by

$$f_d = 2f_1 - f_2, \tag{12}$$

with a corresponding change to (11):

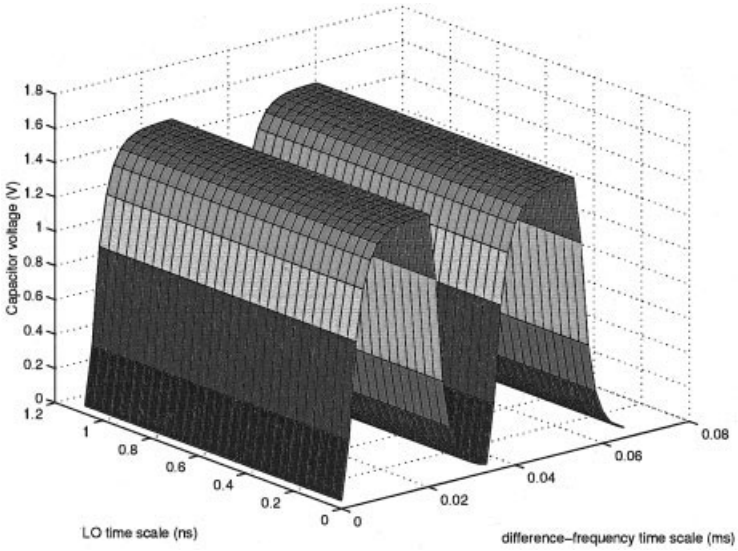

Figure 6. Unbalanced mixer: voltage at capacitor.

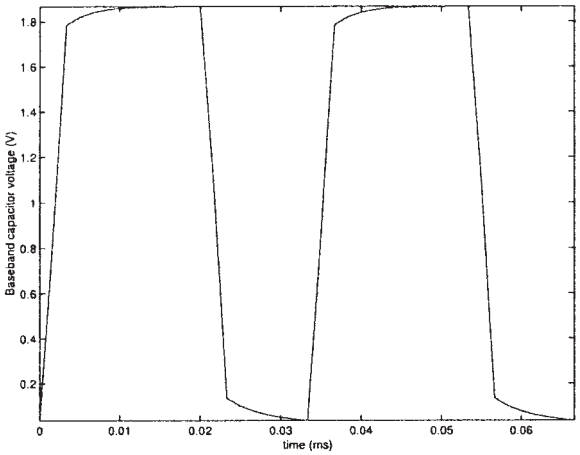

Figure 7. Unbalanced mixer: baseband voltage at capacitor.

$$\hat{z}_2(t_1, t_2) = \hat{z}_s(f_1 t_1, 2f_1 t_1 - f_d t_2), \tag{13}$$

thus restoring the property $z(t) = \hat{z}_2(t, t)$.

An important point to note is that the signals need not be sinusoidal or near-sinusoidal. Indeed, high-frequency "tones" involving modulation by bit streams can be used to drive a circuit. For example, the normalized-to-period-1 information-carrying tone driving the balanced mixer in section IV is given in multitime form by

$$\hat{b}_i(t_{1s}, t_{2s}) = 2\cos(2\pi \times 2t_{1s})\text{pulse}(2(2t_{1s} - t_{2s})), \tag{14}$$

and $\hat{b}_i(f_1 t_1, f_2 t_2)$ is shown in Figure 3.

III. DISCRETIZATION AND NUMERICAL SOLUTION

The MPDE (4), reformulated in terms of sheared-difference time scales as in the previous section, may be solved by any of the numerical methods discussed in [13] for widely-separated time scales. In particular, (4) may be discretized at a set of grid points in the (t_1, t_2) plane in order to obtain a system of equations for the samples of $\hat{x}$ at these grid points. For example, on a rectangular grid, applying an implicit first-order numerical integration scheme to (4) at each grid point $t_1 = t_{1m}$, $t_2 = t_{2n}$ leads to the following equation:

$$(h_1 + h_2)q(\hat{x}_{mn}) - h_2 q(\hat{x}_{m-1,n}) - h_1 q(\hat{x}_{m,n-1}) + h_1 h_2(f(\hat{x}_{mn}) + \hat{b}(t_{1m}, t_{2n})) = 0. \tag{15}$$

In (15), $h_1 = t_{1m} - t_{1,m-1}$, $h_2 = t_{2n} - t_{2,n-1}$, and $\hat{x}_{i,j} = \hat{x}(t_{1i}, t_{2j})$. The collection of these discretized equations over all grid points comprises a set of coupled nonlinear equations, which may be solved numerically with a nonlinear solution algorithm such as Newton–Raphson [11].

The solution of the discretized equations typically involves several iterations of linear equation solution with the Jacobian matrix of the system (15). The form of (15) lends this Jacobian matrix a p-level banded block structure, where the lowest-level blocks are of the size of the circuit and p is the number of time-scales in the MPDE. Figure 4 illustrates the structure of the actual Jacobian matrix for the balanced mixer circuit in section IV. Each visually distinguishable point represents a sparse circuit matrix; the thicker

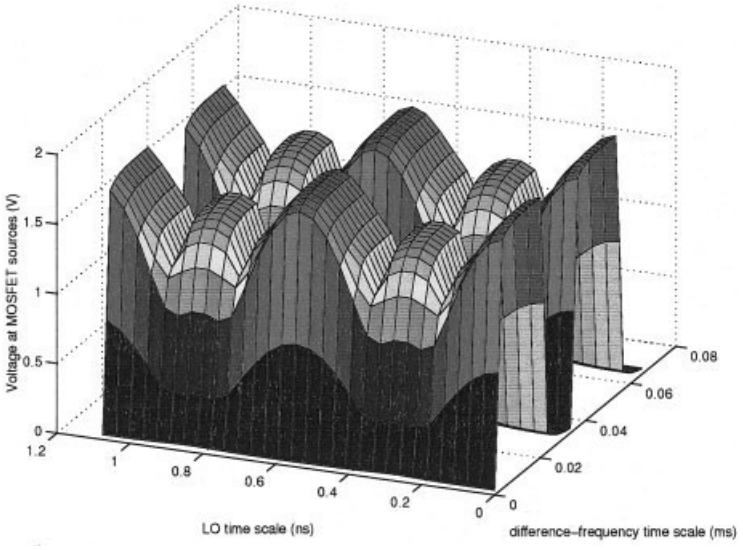

Figure 8. Unbalanced mixer: voltage at MOSFET sources.

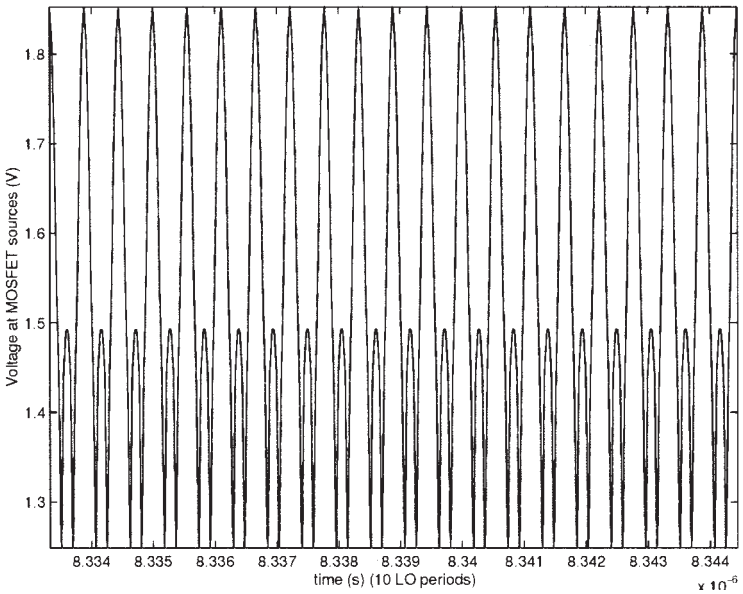

Figure 9. Unbalanced mixer: voltage at MOSFET sources.

bands contain internal block-substructure. Note the band of matrices at the top right corner—these result from the periodicity of (3), as does the fact that each small submatrix in the figure also has a similar wrap-around structure. For large circuits, it is necessary to apply iterative linear solution techniques, similar to approaches in [4, 15], to solve linear systems with the Jacobian matrix. The LU-factorization-based solution leads to a block-column of fill-ins towards the right end of the matrix and is therefore limited to relatively small circuits.

It should also be noted that the convergence of the Newton–Raphson algorithm for a nonlinear solution is far from guaranteed, especially for large circuit problems where it can exhibit a very limited region of convergence. For this reason, homotopy or continuation methods [1, 7], built around a series of locally convergent Newton–Raphson solutions, can be of great benefit in ensuring robust, unattended solution in practice. We have employed a continuation scheme similar to that reported in [14], with uniform success.

IV. APPLICATION AND EXAMPLES

A. Unbalanced CMOS-RF Down-Conversion Mixer

The unbalanced mixer circuit shown in Figure 5 is based on CMOS-RF switching down-conversion cir-

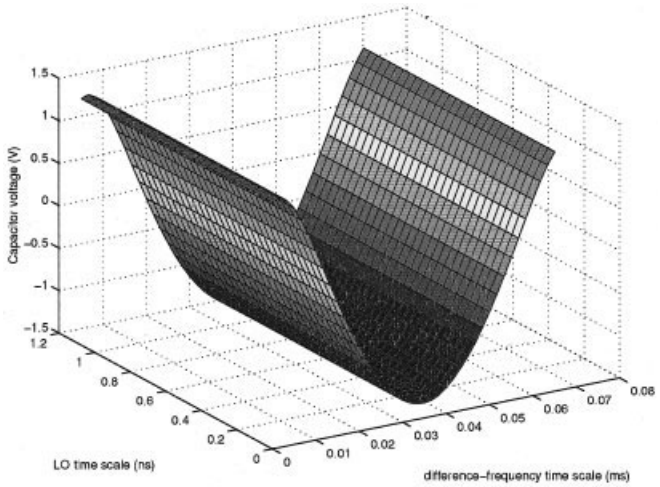

Figure 10. Sinusoidal driving tones, capacitor voltage (V).

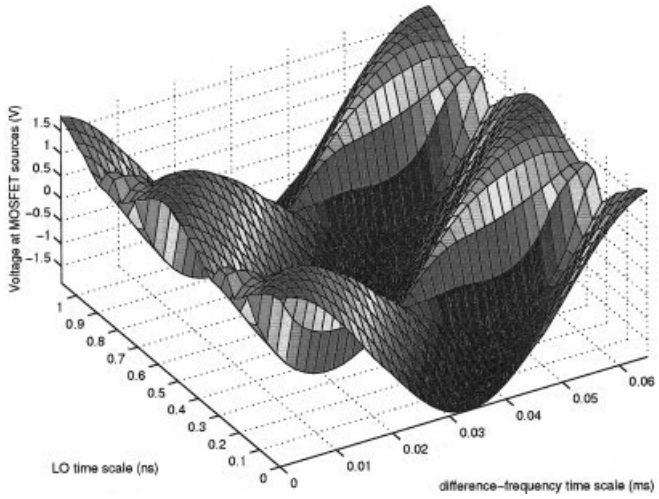

Figure 11. Sinusoidal driving tones, voltage at sources (V).

cuits proposed in [10]. The LO signal was chosen to be a sinusoid at 900 MHz, while the RF signal "tone" was at 900 MHz + 15 kHz. The RF signal was not sinusoidal; instead, it was a 900-MHz sinusoidal tone ideally modulated by two pulses at 15 kHz, representing two bits of a bit stream. During circuit operation, the LO signal switches the two MOSFETs on and off in roughly alternate fashion, thereby down-converting the RF signal to baseband. The low-pass filter formed by the MOSFET's internal resistances and capacitances, together with R and C, results in the baseband signal directly at the capacitor node.

Figure 6 depicts the multitime voltage at the capacitor node upon solution with the new technique. The variation along the difference time scale (with a period of 1/15 kHz) clearly depicts the actual shape of the bits at baseband, including filtering and distortion effects and, potentially, intersymbol interference (ISI) and adjacent-channel interference (ACI) degradations. The lack of variation along the LO time scale indicates the extent to which fast-varying signals have been filtered out. Figure 7 shows a cross-section of the multi-time capacitor voltage along the difference time scale. In the absence of LO variations, it is also the actual baseband voltage at the capacitor. The benefits of time-domain solution, such as the capture of sharp corners and absence of spurious ringing, are apparent. Figure 8 shows the multitime voltage at the node connecting the two MOSFETs. At this point, prior to lowpass filtering, the waveform contains significant variations along both the difference-frequency and LO time scales. Frequency-doubling of the LO, due to the switching action, can be easily discerned in the shape of the waveform as it changes along the LO time scale. Figure 9 depicts a small section (10 periods of the LO) of the actual (normal-time) voltage

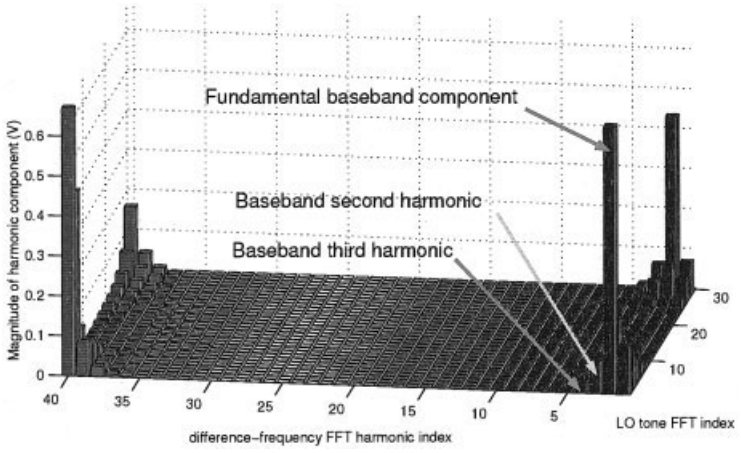

Figure 12. Harmonic components of capacitor voltage (V).

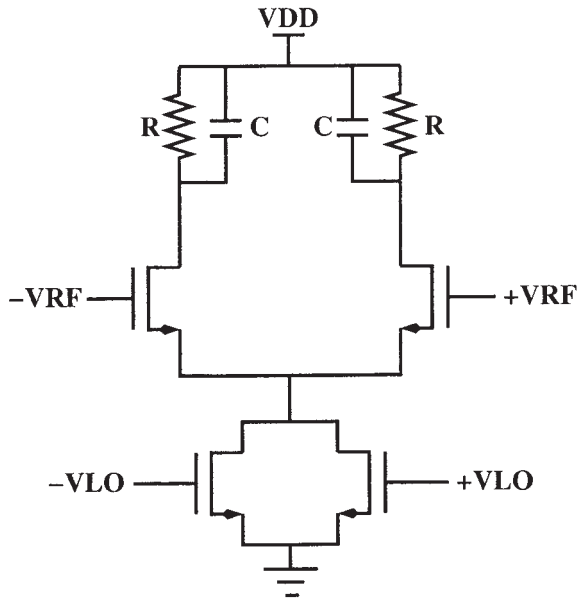

Figure 13. Balanced CMOS down-conversion mixer [10].

waveform at the MOSFET sources, obtained from the multitime voltage using eq. (2).

To estimate the harmonic distortion at baseband, the circuit was solved with sinusoidal driving tones for both LO and RF inputs. Figures 10 and 11 depict the multitime forms of the voltages at the capacitor node and at the MOSFET sources, respectively. The harmonic components of any multitime signal can be obtained by a 2D Fourier series analysis as a post-processing step. Figure 12 shows the results of such an analysis on the capacitor voltage, with the baseband fundamental component and the first two distortion components indicated. It can be seen that small components of the LO frequency are also present.

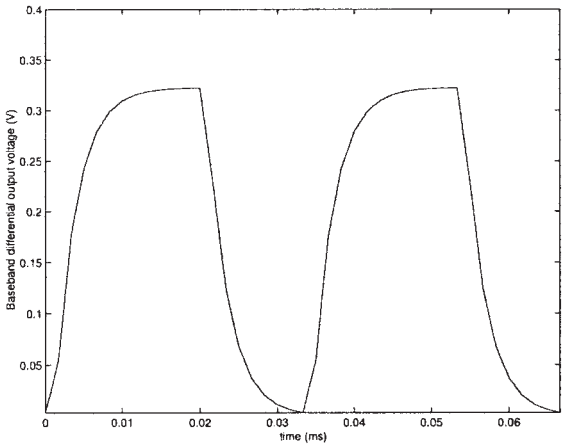

Figure 15. Balanced mixer: baseband differential output.

B. Balanced LO-Doubling Down-Conversion Mixer

The circuit shown in Figure 13 is a balanced mixer, adapted from a circuit proposed in [16]. An important feature of this circuit is that the lower pair of MOSFETs constitutes a frequency doubler, generating a current at twice the LO frequency. This current feeds the differential pair formed by the upper two MOSFETs, thus resulting in mixing and down-conversion. The supplied LO signal in this case is a sinusoid at 450 MHz; the RF signal "tone" is the same as that in the previous circuit, a modulated bit stream close to 900 MHz. For this circuit, the natural choice

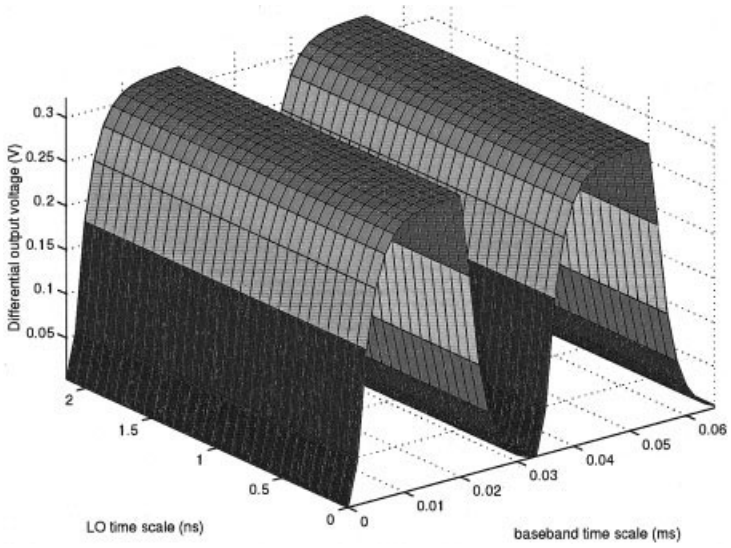

Figure 14. Balanced mixer: differential output voltage.

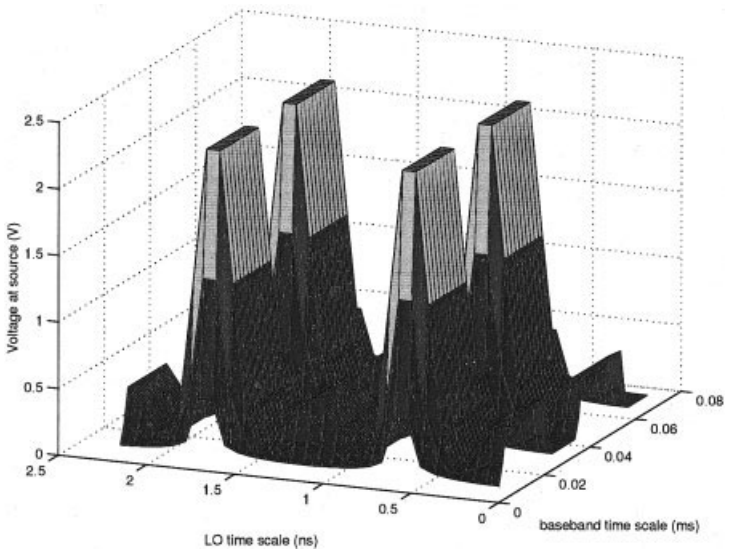

Figure 16. Balanced mixer: voltage at MOSFET sources.

for the difference frequency is given by (12), again resulting in a baseband frequency of 15 kHz. The time-shearing function is given by (13). The multitime form of the differential output voltage between the drains of the upper MOSFETs is shown in Figure 14. Once again, the time-domain shape of the bit stream is evident from the variation along the difference-frequency time scale. Figure 15 shows the envelope along the difference-frequency time scale, corresponding to the actual baseband voltage of the output.

The sharp waveforms created by the action of the frequency doubler in the circuit are clearly visible in Figure 16, which depicts the multitime voltage at the sources of the differential pair. The advantages of fully time-domain solution methods are best utilized in such situations. A small section of the actual voltage waveform, over a period of five LO cycles, is depicted in Figure 17.

C. Computational Speed-up

The computational speed-up of the new method stems from the fact that relatively few grid points in the multitime plane are sufficient to capture solution waveforms, compared to the number of time points needed for normal-time representation. For the balanced mixer circuit above, we employed a 40 $\times$ 30 grid, resulting in 1200 grid points. The wall-clock time for the longest run (26 iterations) of Newton–Raphson on the balanced mixer circuit (given a good starting guess) was 1 m3s.* In cases where Newton–Raphson did not converge, using continuation reliably obtained solutions in 10–20 m.

The closest comparable traditional time-domain approach is shooting (or time-discretization) across one period of the difference frequency, but with time steps small enough to capture the LO variations with sufficient accuracy, that is, 10 or more time steps per LO period. This amounts to some 300,000 or more time steps over the difference-frequency period, resulting in an equation system more than 250$\times$ larger.

* All times are on a single-CPU, 1.4 GHz AMD Athlon system with 512 MB of 133-MHz DDR memory, running Linux 2.4.15.

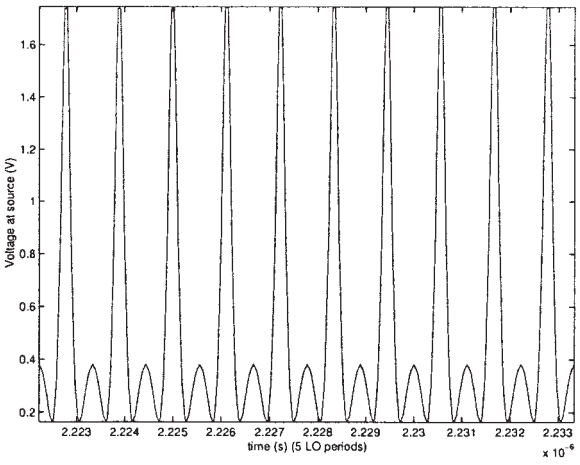

Figure 17. Balanced mixer: voltage at MOSFET sources.

Using iterative linear solution methods and in the presence of similar nonlinear convergence behaviour, this results in a computational advantage of more than two orders of magnitude in favour of the new method described here. However, because it can be significantly more difficult to obtain nonlinear solution convergence for traditional shooting than for the multitime approach in the presence of widely separated time scales, the real user-experienced speed-up can be considerably larger.

We note that the speed-up depends roughly linearly on the extent of the disparity between the LO time scale and the difference-frequency time scale. The break-even point (in terms of frequency separation) for computational speed-up over single-time shooting is strongly dependent on implementation. We have noted that frequency disparities of 200 and above confer a speed advantage to multitime methods.

Furthermore, we note that while the numerical examples in this paper have used a fixed, uniform solution grid for numerical discretization, the method presented is equally applicable to situations where the grid is nonuniform. Indeed, nonuniform grids are useful for adaptation to sharp changes in multitime waveforms.

CONCLUSION

Through the use of sheared difference-frequency time scales, we have extended multitime circuit-solution formulations, previously useful only for widely-separated driving tones, to situations where driving signals are close in frequency. A purely time-domain method for solving the resulting equations has been presented and applied to compute the time-domain shapes of baseband bit-streams in down-conversion mixers. This new method is well suited for estimating effects such as ISI and ACI in communication-symbol streams. When baseband variations are much slower than those of the driving signals, it is also more than two orders of magnitude faster than comparable single-time methods.

ACKNOWLEDGMENTS

The author would like to thank the second anonymous reviewer of this article for a thorough review and insightful suggestions for improvement.

REFERENCES

1. E.L. Allgower and K. Georg, Numerical continuation methods. Springer-Verlag, New York, 1990.
2. T.J. Aprille and T.N. Trick, Steady-state analysis of nonlinear circuits with periodic inputs, Proc IEEE 60 (1972), 108–114.
3. H.G. Brachtendorf, G. Welsch, R. Laur, and A. Bunse-Gerstner, Numerical steady state analysis of electronic circuits driven by multi-tone signals, Electrical Engg 79 (1996), 103–112.
4. D. Long, R.C. Melville, K. Ashby, and B. Horton, Full chip harmonic balance, Proc IEEE CICC, Santa Clara, CA, 1997.
5. R.J. Gilmore and M.B. Steer, Nonlinear circuit analysis using the method of harmonic balance: A review of the art. Pt I: Introductory concepts, Int J Microwave Millimeter Wave CAE 1 (1991).
6. K. Kundert, J. White, and A. Sangiovanni-Vincentelli, A mixed frequency-time approach for distortion analysis of switching filter circuits, IEEE J Solid-State Circ 24 (1989), 443–451.
7. K.S. Kundert, J.K. White, and A. Sangiovanni-Vincentelli, Steady-state methods for simulating analog and microwave circuits, Kluwer Academic, 1990.
8. L.W. Nagel, SPICE2: A computer program to simulate semiconductor ci Ph.D. thesis, University of California, Berkeley, 1975, memorandum no. ERL-M520.
9. J. Parkhurst and L. Ogborn, Determining the steady-state output of nonlinear oscillatory circuits using multiple shooting, IEEE Trans CAD 14 (1995), 882–889.
10. J. Pihl, K.T. Christensen, and E. Braun, Direct down-conversion with switching CMOS mixer, Proc IEEE ISCAS, Sydney, Australia, 2001, pp. I-117–I-120.
11. W.H. Press, S.A. Teukolsky, W.T. Vetterling, and B.P. Flannery, Numerical recipes: the art of scientific computing, Cambridge University Press, Cambridge, 1989.
12. T.L. Quarles, SPICE 3C.1 user's guide, University of California, Berkeley, EECS Industrial Liaison Program, University of California, Berkeley, 1989.
13. J. Roychowdhury, Analysing circuits with widely-separated time scales using numerical PDE methods, IEEE Trans Circ Syst 48 (2001), 578–594.
14. J. Roychowdhury and R.C. Melville, Homotopy techniques for obtaining a DC solution of large-scale MOS Circuits, Proc IEEE DAC, Las Vegas, NV, 1996.
15. R. Telichevesky, K. Kundert, and J. White, Efficient steady-state analysis based on matrix-free Krylov subspace methods, Proc IEEE DAC, San Francisco, CA, 1995, pp. 480–484.
16. Z. Zhang, Z. Chen, and J. Lau, A 900-MHz CMOS balanced harmonic mixer for direct conversion receivers, Proc IEEE Radio Wireless Conf (RAWCON), Denver, CO, 2000, pp. 219–222.

BIOGRAPHY

Jaijeet Roychowdhury received a Bachelor's degree in Electrical Engineering from the Indian Institute of Technology (Kanpur) in 1987, and his Ph.D degree in EECS from the University of California (Berkeley) in 1993. From 1993 to 1995, he was with the CAD Lab of AT&T's Bell Laboratories in Allentown, PA; from 1995–2000, with the Communication Sciences Research Division of Lucent's Bell Laboratories in Murray Hill, NJ; and from 2000–2001, with CeLight, Inc., an optical networking startup in Silver Spring, MD. Since 2001, he has been with the ECE Department and the Digital Technology Center of the University of Minnesota. He received Distinguished or Best Paper Awards at ICCAD 1991, DAC 1997, ASP-DAC 1997, ASP-DAC 1999, and ASP-DAC 2005, and was cited for Extraordinary Achievement by Bell Laboratories. He has served on the Technical Program Committees of DAC, ICCAD, BMAS, SCEE, ASPDAC, and ISCAS, and is an IEEE CAS Society Distinguished Lecturer for the period 2003–2005. He is currently serving as IEEE CAS/CANDE representative to ICCAD's Executive Committee and as Program Chair of IEEEs 2005 BMAS and CANDE workshops. His professional interests include the design, analysis, and simulation of electronic, electro-optical, and mixed-domain systems, particularly for high-speed and high-frequency communications. He holds ten patents.